

Modeling and Simulation of an Industrial Two-Shaft Gas Turbine for the Purpose of Controller Design by Employing Invasive Weed Optimization Method

Morteza Montazeri-Gh, Shabnam Yazdani and Ehsan Mohammadi
Systems Simulation and Control Laboratory, School of Mechanical Engineering,
Iran University of Science and Technology, Tehran, Iran

Abstract: In power industries, the need for an appropriate model within the process of control system design along with the importance of condition monitoring and reducing maintenance costs, increase the demand for development of an accurate model capable of estimating engine dynamic behavior under different working conditions. In this study, an industrial two-shaft gas turbine is modeled and simulated in the Matlab-Simulink environment and a multi-loop controller is designed for it. For this purpose, first, a thermodynamic model of the engine capable of predicting its performance at full and part load conditions is presented. A fuel control system based on min-max control strategy is devised and its parameters are modified utilizing Invasive Weed Optimization algorithm as a powerful global optimization technique. The performance of suggested model in steady-state condition is validated against the data published by the manufacturer and the results obtained confirmed the reliability of the model and its capability in simulating the gas turbine's actual behavior. In order to study the controller's ability in maintaining desired rotational speed of the power turbine shaft, sharp load variations are exerted to the model and the controller's functionality in wide load ranges is analyzed. According to the results, the proposed controller is capable of meeting the expectations.

Key words: Two-shaft gas turbine, modeling and simulation, fuel control system, invasive weed optimization method, Iran

INTRODUCTION

Now a days, gas turbines are one of the most practical power generating systems. Due to high installation and maintenance costs, monitoring of these systems has always been of great importance. Also, design and development of up-to-date and cost efficient systems requires lots of experimental work and great investments. On the one hand, these inefficient experiments and on the other hand, the need for health monitoring and control of gas turbines has attracted the attention to computational tools capable of providing realistic estimations of gas turbine performance, transient operation analysis, control systems design or the study of critical operational modes.

Dynamic models of gas turbines are combinations of algebraic equations and first order ordinary differential equations resulted from exerting principles like conservation of mass, energy and momentum to each component of the engine. So far, many methods have been developed for dynamic modeling of gas turbines. These methods vary from simple models to complex ones based on the application of the model. During transient

operation, in order to obtain an adequate response from the model, automatic control systems capable of satisfying operating limitations as well as considering physical constraints of the system must be designed.

Initially, gas turbines were modeled in first order linear forms (Cohen *et al.*, 1966). In these early models, the relationship between fuel mass flow entering the combustion chamber and rotational speed of the shaft was the only parameter determining system's dynamics. Due to the limitations of the linear models, researchers aimed for nonlinear, more accurate models. The first nonlinear model of a gas turbine was presented by Saravanamuttoo and Fawke (1970). Hence, these models have evolved from the first simplified schemes (Fawke *et al.*, 1972) to frequency domain analysis (Rowen, 1983) and time domain simulations (Camporeale *et al.*, 2002; Kim *et al.*, 2001a).

The complex models were accurate but slow, therefore nonlinear models were linearized and real-time models were introduced (Rao *et al.*, 1990). In these models, state-space representation or transfer functions were mainly used for simulating transient behavior of gas turbines. System identification is another successful

method of dynamic modeling, and block-diagram models such as Wiener (Schetzen, 1981) place in this category. One of the most recent approaches in this field is presented by Mohammadi and Montazeri-Gh (2014) for the gray-box identification of Wiener models.

As the output of linear models is acceptable only in a limited area adjacent to the design point, piecewise-linear models were developed in which linearization is performed around several operating points (Breikin *et al.*, 2004). Quasi-linear models are another type of nonlinear models made up from quasi-linear differential equations and nonlinear algebraic equations, claimed to maintain good accuracy in case of severe input variations (Lichtsinder and Levy, 2006).

A complete model of gas turbine engine can be developed from its geometry or performance maps (Cohen *et al.*, 1966). In more complex models, one-dimensional equations are used to analyze compressors. In order to include the effects of inter-stage bleeding, Variable Inlet Guide Vanes (VIGV) and Variable Stator Vanes (VSV) modulation, these equations are derived from integral conservation and applied stage by stage on the compressor map, obtaining corrected curves (Kim *et al.*, 2001b; Chacartegui *et al.*, 2011). Analysis on start-up of heavy gas turbines (Kim *et al.*, 2002) and combined cycle dynamic analysis utilizing constant geometry compressor curves (Kim *et al.*, 2001) are also some extensions of gas turbine dynamic modeling.

Various control strategies have been used in design process of control systems for gas turbines and power plants. Rowen (1983) presented a control system based on a proportional integral speed governor, suitable for heavy-duty engines. Kim *et al.* (2001) modified this scheme for both small and heavy duty gas turbine dynamic models. In these cases, proportional integral derivative speed governors were used to regulate the fuel mass flow. In recent years, more complex control systems such as fuzzy logic controllers capable of solving some recurrent issues found with conventional PIDs have been suggested (Nelson and Lakany, 2007; Jafri and Montazeri-Gh, 2011; Mohammadi *et al.*, 2013). Multi-objective controllers using genetic algorithms (Chipperfield and Fleming, 1996), Optimal LQR controllers (Camporeale *et al.*, 1997) and adaptive PID controllers (Wang *et al.*, 2008) are also examples of gas turbine control systems designed for satisfying desired engine operating conditions. Jafarian *et al.* (2016) proposed the application of multi-objective optimization algorithm, called multi-objective particle swarm optimization, in optimizing the setting of the valves in the gas turbine. Mehrian provided very prominent results in thermal analysis of different materials under thermal shock. He

provided novel methods to calculate strain energy and a new algorithm to optimize material properties (Mehrian *et al.*, 2013; Nowruzpour Mehrian, 2014; Mehrian and Mehrian, 2015, 2016).

In this study, a dynamic simulation code for two-shaft industrial gas turbines is provided in Matlab-Simulink environment. For this purpose, first, a nonlinear thermodynamic model of gas turbine is developed. Then, a multi-loop fuel control system based on the min-max strategy is designed and its parameters are optimized utilizing the Invasive Weed Optimization (IWO) algorithm. It is shown that the min-max controller complies with requirements of gas turbine operating conditions.

Present study is structured in five parts. The first part deals with gas turbine mathematical modelling, the second part describes the design point, off-design and transient solving strategy. In the third part, a controller based on min-max strategy is designed and its parameters are optimized by IWO algorithm. Simulation results along with validation of the model against real operating data at stationary design and off-design conditions are presented in the fourth part. Finally, the dynamic behavior of the engine and controller's performance is evaluated under different situations and main conclusions are given.

MATERIALS AND METHODS

Gas turbine mathematical modeling: Thermodynamic modeling of gas turbines takes place in three steps which are respectively known as design point, off-design and transient modeling. In component by component modeling approach, mathematical models of individual components including compressor, combustor and turbines are developed and integrated in a simulating tool (Chacartegui *et al.*, 2011). Design point modeling will determine unknown parameters at this point. The rotor speed is constant at each steady-state working point.

These points are indicative of working conditions at different rotor speeds and together form the running line of the engine. The steady-state points are evaluated from the power balance equation between compressor and gas generator turbine. External factors such as variation of input load will disturb the balance and initiate transient mode. In this section, each component's governing equations are derived and modeling methodology is described.

Thermodynamic properties of gas: Due to the dependency of gas properties on its temperature and composition, specific heat of working fluid and gas constant (R) vary throughout the engine. Specific heat is

defined by a polynomial function with constant coefficients (Walsh and Fletcher, 2004). The gas constant (R) for dry air is a fixed value, but for combustion products changes according to the type of fuel and the fuel to air ratio. In case of dry air, specific heat capacity is only a function of temperature while for air and fuel mixture, it is dependent on both temperature and fuel to air ratio. It should be noted that both gas constant and specific heat are dependent on the pressure of the fluid, but due to the slight effect of pressure in comparison to temperature, pressure related terms can be neglected.

Compressor model: During transient mode, compressor is assumed to have a quasi-steady behavior and its performance is analyzed with steady-state characteristic map. Compressor map is a graph generated from integral of stage characteristics. Stage diagrams are normally represented by plotting stage loading coefficient against flow coefficient. These coefficients are determined based on stagnation enthalpy, blade velocity and axial fluid velocity. Overall characteristic map is achieved utilizing stage stacking method. Turbo-machinery characteristic maps are produced on a non-dimensional basis but instead of using stage loading and flow coefficients, corrected air mass flow, corrected rotor speed, overall pressure ratio and isentropic efficiency are plotted in a non-dimensional basis. Total air mass flow and rotational speed are corrected according to Eq. 1 and 2:

$$W_{corr} = \dot{m} \frac{P_{ref}}{P} \sqrt{\frac{T}{T_{ref}}} \quad (1)$$

$$N_{corr} = \frac{N}{\sqrt{\frac{T}{T_{ref}}}} \quad (2)$$

Where:

- m = The fluid mass flow in $kg \text{ sec}^{-1}$
- T and T_{ref} = The stagnation and reference temperature in Kelvin
- P and P_{ref} = The stagnation and reference pressure in kpa

Compressors efficiency under different working conditions is illustrated as constant isentropic efficiency curves on the map. Equation 3 illustrates the relationship between temperature and pressure of a fluid entering and exiting a compressor:

$$T_{out} - T_{in} = \frac{T_{in}}{\eta_c} \left[\left(\frac{P_{out}}{P_{in}} \right)^{\frac{\gamma-1}{\gamma}} - 1 \right] \quad (3)$$

Where:

- γ = The specific heat ratio
- η_c = the compressor's isentropic efficiency obtained from the map

By knowing inlet temperature and pressure values, reading compressor isentropic efficiency from the map and calculating output pressure, output temperature will be computed and thus compressor's required power can be evaluated from Eq. 4:

$$W_c = \dot{m}_{air} [(c_{p,out} T_{out}) - (c_{p,in} T_{in})] \quad (4)$$

In order to prevent surge effects in full loading, variable inlet guide vanes are used to control the air flow passing through compressor (Turie, 2011). In other words, compressor's characteristic map is modified with a correcting coefficient. At high speeds, variable inlet guide vanes are fully open. As rotor accelerates, in order to control turbine exhaust temperature, the angle of guide vanes and the fuel mass flow entering combustion chamber change according to rotational speed.

Equation 5 and 6 are experimental formulas used for obtaining Correction Coefficients (CCO) of air mass flow, Pressure Ratio (PR) and efficiency. Design parameters are multiplied by correction coefficients and a new map is achieved for the compressor. Other parameters can be evaluated utilizing the map and corrected values (Gilani *et al.*, 2009):

$$PR_{CCO} = \dot{m}_{CCO} = (2.9066e-03)\alpha + 0.8197 \quad (5)$$

$$\eta_{CCO} = (1.6666e-04)\alpha + 0.9896 \quad (6)$$

where (α) is the percentage of VIGVs openings.

Combustor model: Conservation of mass and energy are the two laws governing the fluid passing through combustion chamber. Conservation of mass states that the difference between the total mass entering the combustor and exiting it is equal to the change of total mass of gases inside the combustor at each time step (Eq. 7):

$$V_{CC} \frac{d\rho}{dt} = \dot{m}_{air} + \dot{m}_{fuel} - \dot{m}_{gas} \quad (7)$$

As illustrated in Eq. 8, conservation of energy states that the change of fluid energy with time is equal to the difference between the energy of fluid entering and exiting the combustion chamber:

$$\frac{d(M_{cc}U_{cc})}{dt} = \dot{m}_{air}h_{air} + \dot{m}_{fuel}(h_{fuel} + LHV\eta_{cc}) - \dot{m}_{gas}h_{gas} \quad (8)$$

Where:

- LHV = The low heating value of the fuel in kJ kg^{-1}
- M_{cc} = The total mass of gas in burner in kg
- U_{cc} = The internal energy of the gas in kJ
- η_{cc} = The combustion chamber efficiency

The M_{cc} depends on outlet pressure, outlet temperature and the composition of gas and it is calculated from the ideal gas equation under the assumption of complete combustion of fuel to carbon dioxide, water steam, nitrogen and oxygen (Chacartegui *et al.*, 2011). Combustion chamber exhaust gas temperature and the density of flowing fluid are considered time variant. Pressure and temperature of the gas inside the burner are considered to take the same values as exhaust pressure and temperature at all points. Combustion chamber is assumed to be a control volume with heat and mass transfer only in boundaries. Based on these assumptions, Eq. 8 can be rewritten as Eq. 9:

$$\dot{m}_{gas}c_{p, gas} \left(\frac{M_{cc}}{\gamma \dot{m}_{gas}} \right) \frac{dT_{gas}}{dt} = \dot{m}_{air}h_{air} + \dot{m}_{fuel}(h_{fuel} + LHV\eta_{cc}) - \dot{m}_{gas}h_{gas} \quad (9)$$

Efficiency for gas turbines combustors is in range of 98-99.9% and can be estimated from experimental equations in off-design operations (Walsh and Fletcher, 2004). Pressure loss along burner is calculated from Eq. 10. By knowing the amount of pressure loss in design point, the pressure loss in other working points can be derived:

$$\left(\frac{\Delta P}{P} \right) \approx \left(\frac{\dot{m}\sqrt{T}}{P} \right)^2 \quad (10)$$

Turbine model: In case of two-shaft gas turbines, the energy resulted from pressure loss in high pressure turbine which is also called as Gas Generator Turbine (GGT) is fed to compressor and engine accessory systems. Low pressure turbine is connected to another shaft and its power is delivered to consumers and therefore is called Power Turbine (PT). The power generated in a turbine is evaluated by Eq. 11:

$$W_{Turb} = \dot{m}_{gas} [(c_{p, in} T_{in} - c_{p, out} T_{out})] \quad (11)$$

Like compressors, turbines characteristics are also presented in a non-dimensional basis. Flow and speed in

turbines are corrected by the same equations used for compressors. Turbine characteristic map is a graph relating pressure ratio to corrected mass flow and isentropic efficiency in different corrected speeds. Increase in pressure ratio will raise the mass flow to a certain amount. At this point, turbine is choked and the change in speed will cause a slight change in corrected mass flow. By knowing pressure ratio and isentropic efficiency of turbine, exhaust gas temperature will be obtained from Eq. 12:

$$T_{in} - T_{out} = \eta_T T_{in} \left[1 - \frac{1}{\left(\frac{P_{in}}{P_{out}} \right)^{\frac{\gamma-1}{\gamma}}} \right] \quad (12)$$

Solving strategy: Mathematical equations of gas turbine components are not independent and there is only one solution that satisfies all at the same time. In order to obtain this solution, we need a solving strategy. This unique solution will be determined by iteration through algorithm loops. In modeling of two-shaft gas turbines, there are two main constraints that must be satisfied; first, the power balance equation between compressor and gas generator turbine (Eq. 13) which states that at each steady-state working point, the power generated by turbine must be equal to the power consumed by compressor:

$$\frac{(T_{out} - T_{in})_{comp}}{T_{in, comp}} = \eta_{mech} \frac{(T_{in} - T_{out})_{GGT}}{T_{in, GGT}} \frac{T_{in, GGT}}{T_{in, comp}} \frac{c_{p, gas}}{c_{p, air}} \quad (13)$$

The second constraint is the compatibility equation between turbines (Eq. 14). Although, there is no mechanical connection between the gas generator and the power turbine, an aerodynamic coupling exists between these two components. In average and high power applications, power turbine is choked. At this state, the fluid mass flow passing through power turbine is constant and must be equal to the mass flow exiting gas generator turbine.

In other words, power turbine's input capacity controls gas generator turbine's pressure ratio. Pressure ratio of gas generator remains constant as long as power turbine is choked. In low power applications, power turbine is not choked anymore and gas generator's pressure ratio decreases. This pressure drop is necessary for maintaining compatibility between turbines:

$$\left(\frac{\dot{m}\sqrt{T_{in}}}{P_{in}} \right)_{PT} = \left(\frac{\dot{m}\sqrt{T_{in}}}{P_{in}} \times \frac{P_{in}}{P_{out}} \times \sqrt{\frac{T_{out}}{T_{in}}} \right)_{GGT} \quad (14)$$

Equation 15 and 16 illustrate the conservation of angular momentum exerted to Gas Generator Turbine (GGT) and Power Turbine (PT) rotors. The (GGT) rotor connects compressor to gas generator turbine and the (PT) rotor couples power turbine to applied loading:

$$I_{GGT}\omega_{GGT} \frac{d\omega_{GGT}}{dt} = \eta_{mech} W_{GGT} - W_C - W_{AUX} \quad (15)$$

$$I_{PT}\omega_{PT} \frac{d\omega_{PT}}{dt} = \eta_{mech} W_{PT} - W_{PT} - W_L - W_{AUX} \quad (16)$$

Where:

- I_{GGT} and I_{PT} = The moments of inertia of rotors
- ω_{GGT} and ω_{PT} = The shaft rotational speeds in rpm
- W_{GGT} and W_C = The power produced by the gas generator turbine and the power consumed by compressor in W , respectively
- η_{mech} = The denotes mechanical efficiency of both the gas generator and power turbine's rotors
- W_{PT} , W_{AUX} and W_L = The power produced by the power turbine, engine power loss and the power consumed by load in W

By calculating the angular acceleration, angular velocity at the next time instant ($t+dt$) will be evaluated from Eq.(17, assuming that acceleration is constant in the interval (dt) (Walsh and Fletcher, 2004):

$$\omega(t + dt) = \omega(t) + \left(\frac{d\omega}{dt}\right)\Delta t \quad (17)$$

If (dt) is small enough, by knowing values of rotational speed at time t , moments of inertia of the shafts, and produced and consumed power, rotational velocity of the shaft at time ($t+dt$) can be obtained from Eq. 18:

$$N(t + dt) = N(t) + \frac{\Delta W}{IN(t)} \left(\frac{60}{2\pi}\right)^2 \Delta t \quad (18)$$

Design point modeling: The gas turbine studied in this article is the industrial Siemens Gas Turbine 600 (SGT-600). The SGT-600 is a two-shaft gas turbine with a ten-stage compressor whose first two stages have variable guide blades. The annular combustor accommodates 18 burners. Due to relatively low weight of this gas turbine, it is a good choice for both mechanical drive and power generation applications (Navrotsky and Blomstedt, 2008). Design point properties of this engine are given in Table 1.

Table 1: Design point characteristics of studied gas turbine

Property	Value
Exhaust gas flow (kg sec ⁻¹)	80.4
Net output power (kW)	24800
Heat rate (kJ.kW h ⁻¹)	10535
Compressor pressure ratio	14:1
Exhaust gas temperature (°C)	543
GGT rotor speed (rpm)	9770
PT rotor speed (rpm)	7700

Steady-state modeling: First step of modeling strategy is to select a desired rotational speed for gas generator rotor. Pressure ratio of compressor is guessed at the beginning of an iteration loop and by these two parameters, corrected air mass flow and isentropic efficiency of compressor are interpolated from the map. So far, all properties at compressor outlet including exhaust temperature and pressure are defined. By calculating the pressure loss in burner, its output pressure is evaluated. At this point, exhaust gas temperature is guessed in another iteration loop and the fuel mass flow is calculated utilizing conservation of mass in combustor. Then, corrected gas flow is estimated and is utilized along with gas generator rotor corrected speed to interpolate values of pressure ratio and isentropic efficiency from the map. By knowing all the properties of gas generator turbine outlet, its temperature is obtained.

Now the exhaust temperature of burner is calculated again using compatibility equation and is compared to its initial value. This continues until the error tends to zero. Next, with calculation of power turbine pressure ratio and considering the fact that power turbine rotor speed is constant and equal to design value during steady-state operation, corrected mass flow and isentropic efficiency of power turbine are interpolated from its characteristic map. If the amount of mass flow derived from the map is equal to the value calculated from compatibility equation, the pressure ratio guessed for compressor is confirmed and otherwise, another pressure ratio will be chosen and the loop will start over.

Transient modeling: When the loading on power turbine shaft is changed, in order to maintain operational and physical restrictions, controller changes the amount of fuel mass flow. Thus, the power balance between compressor and gas generator turbine is lost, and a transient phase is initiated. This power difference generates a momentum which causes angular acceleration in rotor.

At the beginning of transient modeling, the compressor pressure ratio is guessed and values of corrected mass flow and isentropic efficiency are interpolated from the map. Burner's exhaust gas temperature is determined from Eq. 9. Next, knowing the corrected mass flow and rotor speed of gas generator

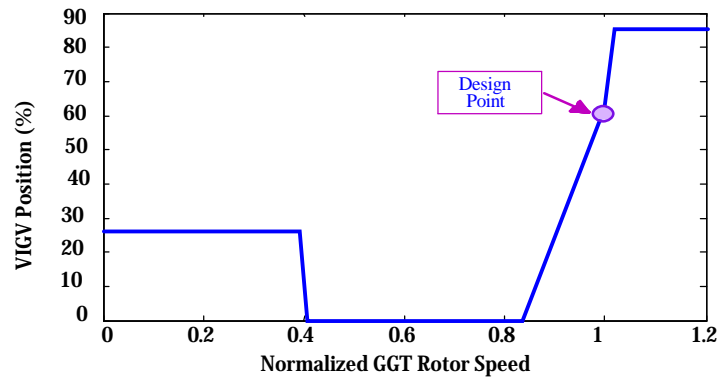


Fig. 1: Variable inlet guide vanes position against normalized GGT rotor speeds

turbine, its pressure ratio and isentropic efficiency are interpolated and all the gas properties at power turbine inlet are determined. Power turbine pressure ratio is calculated and properties of the gas at power turbine outlet are interpolated. The final step is to calculate new rotor speeds and see whether the compatibility equation is satisfied or not. Also, according to the information provided by the manufacturer, change in compressor's inlet guide vanes is only dependent on the corrected gas generator turbine shaft speed (Fig. 1). Noting that the change in load determines the amount of fuel fed to the engine and considering the fact that it is the controller's responsibility to apply these changes, gas turbine dynamic behavior in a closed loop form and in existence of a control system will be studied.

Control strategy: In power generation applications, the aim is to keep power turbine rotor speed or frequency of the shaft at a constant value. In order to achieve this goal, any variations in loading will result in change of gas generator turbine output power and consequently the fuel mass flow and gas generator rotor speed. If the rate of change in gas generator rotor speed violates the limitations, problems including surge in compressor or flame-out in combustor may occur. It is controller's responsibility to guarantee safe performance of the system. This includes limitation of rotational speeds and accelerations as well as physical restrictions such as maximum exhaust gas temperature (Nordstrom, 2005).

During years, many control methods have been used in gas turbine systems. In this study, design process of the gas turbine controller is based on a selection approach between several control loops. This strategy is called "min-max selection strategy" which is an industrial method used in design of gas turbine fuel control systems. Selection of dominant control loop in this unit is based on a min-max approach between transient control loops (Montazeri-Gh *et al.*, 2011).

The min-max controller designed in this research consists of six transient control loops which are power turbine speed control, power turbine acceleration control, gas generator turbine speed limiter, exhaust gas temperature limiter, gas generator turbine acceleration control and gas generator turbine deceleration control. Proportional, Integral and derivative gains are involved in design of power turbine speed and acceleration control loops, while other loops contain a single proportional gain. There is also an open steady-state control loop that prevents flame-out and provides steady-state fuel supply at each gas generator rotor speed from data derived in steady-state modeling. The last variable involved in the control system is the position of inlet guide vanes which is an indirect measurement of the amount of air flowing through the engine. The air mass flow is controlled in an open loop fashion based on the data presented in Fig. 1.

The scheme of the min-max control strategy is shown in Fig. 2. The transient fuel mass flow is evaluated through control loops and added to the steady-state fuel flow. First, among the five control loops mentioned above, the one with minimum output value is selected. In other words, the loop which demands least fuel mass flow takes over the control. The winning loop is then compared to gas generator turbine deceleration control loop and the maximum value is selected. This prevents flame-out in case that sudden drop in fuel to air ratio occurs.

Controller design and optimization: The controller gain tuning is a challenging issue in designing a multi-loop control system. Due to nonlinear and switching nature of this control method, gradient-based optimization techniques show weak results in gain tuning problem and thus a non-gradient based optimization method on the basis of evolutionary algorithms might be a proper choice (Montazeri-Gh *et al.*, 2011). In this study, the controller gains of the presented min-max controller are tuned

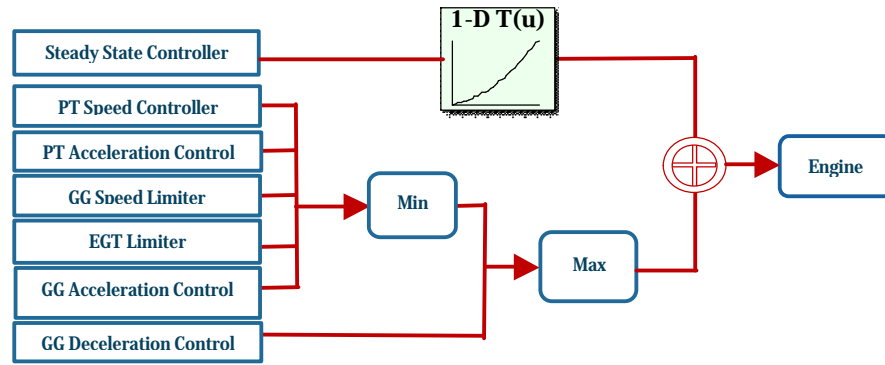


Fig. 2: Scheme of the min-max control strategy

utilizing Invasive Weed Optimization (IWO), a numerical stochastic optimization algorithm inspired from colonizing weeds which was first introduced by Mehrabian and Lucas (2006).

Simulation of colonizing behavior of weeds is proceeded in four steps. First, a population of initial solutions is being spread over the dimensional problem space with random positions. At reproduction, a member of the population of plants is allowed to produce seeds depending on its own and the colony's lowest and highest fitness. Randomness and adaptation in the algorithm is provided in the third part. The generated seeds are randomly distributed over the dimensional search space by normally distributed random numbers with mean equal to zero, but varying variance. This means that seeds will be randomly distributed such that they abode near to the parent plant. However, standard deviation of the random function will be reduced from a previously defined initial value, $\sigma_{initial}$, to a final value, σ_{final} , in every generation. According to Mehrabian and Lucas (2006) nonlinear alteration as give in form of Eq. 19 has shown satisfactory performance:

$$\sigma_{iter} = \frac{(iter_{max} - iter)^n}{(iter_{max})^n} (\sigma_{initial} - \sigma_{final}) + \sigma_{final} \quad (19)$$

Where:

$iter_{max}$ = The maximum number of iterations

σ_{iter} = The standard deviation at present time step and n is the nonlinear modulation index

Last step is competitive exclusion. When the maximum number of weeds in a colony is reached, each weed is allowed to produce seeds according to the mechanism mentioned in reproduction. The produced seeds are then allowed to spread over the search area. When all seeds have found their position in the search area, they are ranked together with their parents. Next, weeds with lower fitness are eliminated to reach the maximum allowable population in a colony.

Table 2: Setting parameters intended for the IWO algorithm

Quantity	Values
No. of initial population (N_0)	15
Maximum no. of plant population (P_{max})	25
Maximum no. of seeds (S_{max})	4
Minimum no. of seeds (S_{min})	1
Nonlinear modulation index (n)	3
Initial value of standard deviation ($\sigma_{initial}$)	1
Final value of standard deviation (σ_{final})	0.01
Maximum no. of iterations ($iter_{max}$)	100

In this way, plants and offspring are ranked together and the ones with better fitness survive and are allowed to replicate.

This mechanism give a chance to plants with lower fitness to reproduce and if their offspring has a good fitness in the colony then they can survive. The population control mechanism also is applied to their offspring to the end of a given run, realizing competitive exclusion. The parameters of the optimization algorithm are listed in Table 2. The solution will stop when the maximum allowable iteration is reached.

Design variables are parameters used for optimization of the objective function. In present study, control gains are determined as variables, generating a 10 dimensional optimization problem. The aim of optimization is to minimize the objective function defined in Eq. 20:

$$J = \frac{1}{w_1 + w_2} \left(w_1 \int_0^{ST} \frac{|N_{des} - N(t)|}{Norm_1} dt \right) + \frac{1}{w_1 + w_2} \left(w_2 \frac{|N_{des} - N_{ss}|}{Norm_2} \right) + \alpha \int_0^{ST} \frac{|E_{\dot{N}(t)}|}{Norm_3} dt \quad (20)$$

Where:

$N(t), N_{des}, N_{ss}$ = The gas generator rotational speed, desired speed and steady-state speed at time (t)

w_1, w_2 = The weight factors

(Norms = The normalization coefficients

α = The penalty coefficient

ST = The total simulation time

$E_{\dot{N}dot}$ = The acceleration error, respectively

RESULTS AND DISCUSSION

In this study, the results of modeling and simulation of the examined two-shaft gas turbine are presented. For this purpose, first, the results of the design point and steady-state modeling are given and validation of the model at off-design stationary conditions is presented afterwards. Next, the results of the invasive weed optimization algorithm are given and finally the performance of the thermodynamic model is evaluated in the presence of the min-max controller and the results obtained are discussed. It should be noted that in addition to the weed algorithm applied in this research, there are other multi-objective evolutionary algorithms such as NSGA-II (modified and utilized in Li *et al.*, 2016; Mobin *et al.*, 2015), NSGA-III and MOPSO (Tavana *et al.*, 2016), ABC algorithm (Vafadrnikjoo *et al.*, 2015) and the general variable neighborhood search algorithm (Komaki *et al.*, 2015), that can be applied in our case problem.

Design point and steady-state modeling results: In the design point modeling of the studied gas turbine, (LHV) of natural gas is considered to be 50030 kJ kg⁻¹. The pressure loss in combustor is assumed to be 5% and its efficiency at design point is considered to be 99.5%. The air entering gas turbine is assumed to be in standard condition with pressure of 101.325 kpa, temperature of 288 K and 60% humidity. After the mathematical model of system is derived, an algorithm for evaluation of design point unknown parameters such as the burner's exhaust gas temperature and the fuel mass flow is developed in Matlab Software. The results of design point modeling for the studied gas turbine are given in Table 3.

The results of the off-design modeling are also illustrated in this section. Figure 3 shows compressor characteristic map and the running line of gas turbine which is obtained by connecting steady-state points. Figure 4a-d and 5a-d illustrate gas generator turbine and power turbine maps, respectively. In high rotational speeds, power turbine is choked and gas generator turbine's pressure ratio remains constant. By reduction of power turbine's inlet gas flow, gas generator's pressure ratio decreases in order to maintain compatibility between turbines. The normalized Compressor Exhaust Temperature (CET), gas generator Turbine Inlet Temperature (TIT), gas generator Turbine Exhaust Temperature (TET) and power Turbine Exhaust temperature (EGT) are shown in Fig. 4. Figure 4a-d illustrates the normalized gas generator speed against normalized fuel mass flow.

Table 3: Results of design point modeling

Quantity	Values
Compressor exhaust temperature (K)	659.1
Compressor isentropic efficiency	0.8057
Compressor consumed power (kW)	32544
Fuel mass flow (kg. sec ⁻¹)	1.5212
Combustor exhaust gas temperature (K)	1381.6
GGT pressure ratio	3.3787
GGT exhaust gas temperature (K)	1041
GGT isentropic efficiency	0.8854
GGT generated power (kW)	32587
PT pressure ratio	3.1795
PT exhaust gas temperature (K)	816
PT isentropic efficiency	0.8853

Validation of model at off-design conditions: In order to validate the prepared model, variations of the exhaust gas temperature (Fig. 5a), exhaust gas flow (Fig. 5b) and output power (Fig. 5c) in off-design conditions and in various environmental temperatures are evaluated and the results are compared to the real off-design data provided by the manufacturer. Figure 5d shows the error between the simulation results and the real data. Maximum difference between the real data and the simulation results is a 3.1% error in output power at environmental temperature of -20°C.

Control system and transient performance analysis: In gas turbine modeling, decent choice of time step plays a great role in accurate transient behavior estimation. A time step of 0.05 sec was considered in transient simulation of studied gas turbine. As mentioned before, the change in gas turbine loading will initiate transient mode. In optimization process, controller command was considered to be a step transition from peak load to 50% load, accompanied by a subsequent transition from 50% load to peak within an interval of 10 sec as shown in Fig. 6a, b.

In order to evaluate the performance of the model in presence of control system, two varying load signals, Figure 6a, were applied to the gas turbine model. First, starting from design condition, a step load rejection of 50% at t = 2 sec was simulated. The 8 sec later, a load rising step was applied bringing back the power to full load. After that, the same procedure was applied with a ramp load variation in order to evaluate the transient model behavior under different working conditions.

Figure 6b illustrates the variation of Fuel Mass Flow (FMF), the control signal sent by the controller to the fuel system. Variations of the gas generator shaft speed, air mass flow and the pressure ratio of compressor are described on compressor map in Fig. 7a, b for step and ramp load variations, respectively. It can be shown that the control system prevents losing surge margin

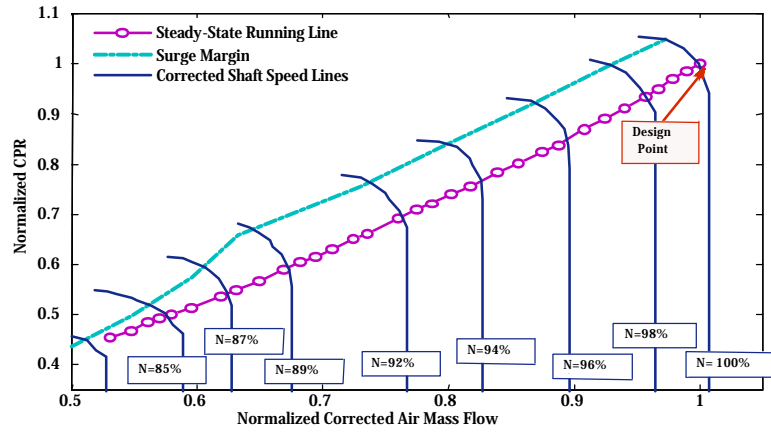


Fig. 3: Compressor characteristic map; steady-state running line

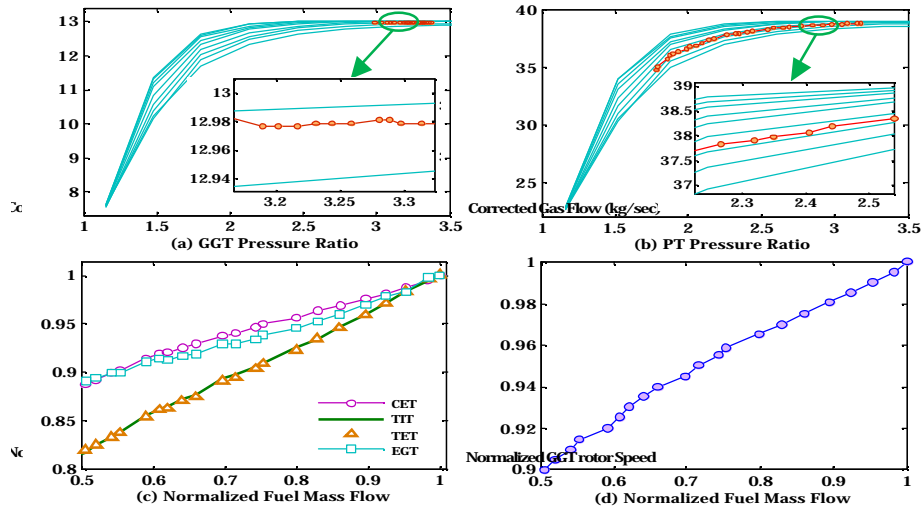


Fig. 4: Simulation results in the steady-state operation: a) GGT map; b) PT map; c) Normalized station temperatures; d) Normalized GGT rotor speed

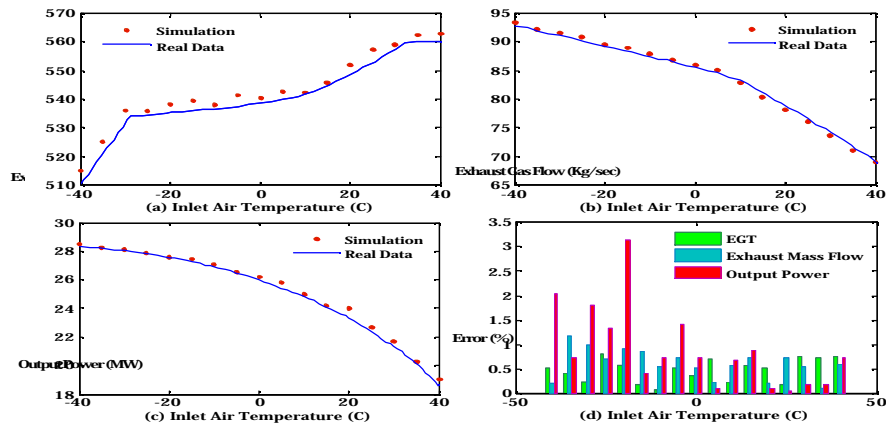


Fig. 5: Model validation at off-design conditions: a) Exhaust gas temperature; b) Exhaust gas flow; c) Output power; d) Error percentage

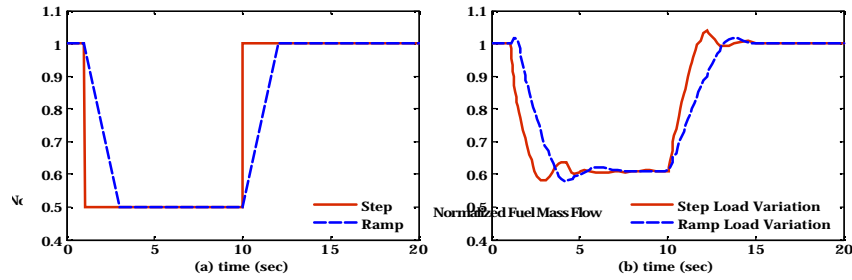


Fig. 6: Transient simulation results in presence of min-max controller: a) Normalized input load; b) Normalized fuel mass flow

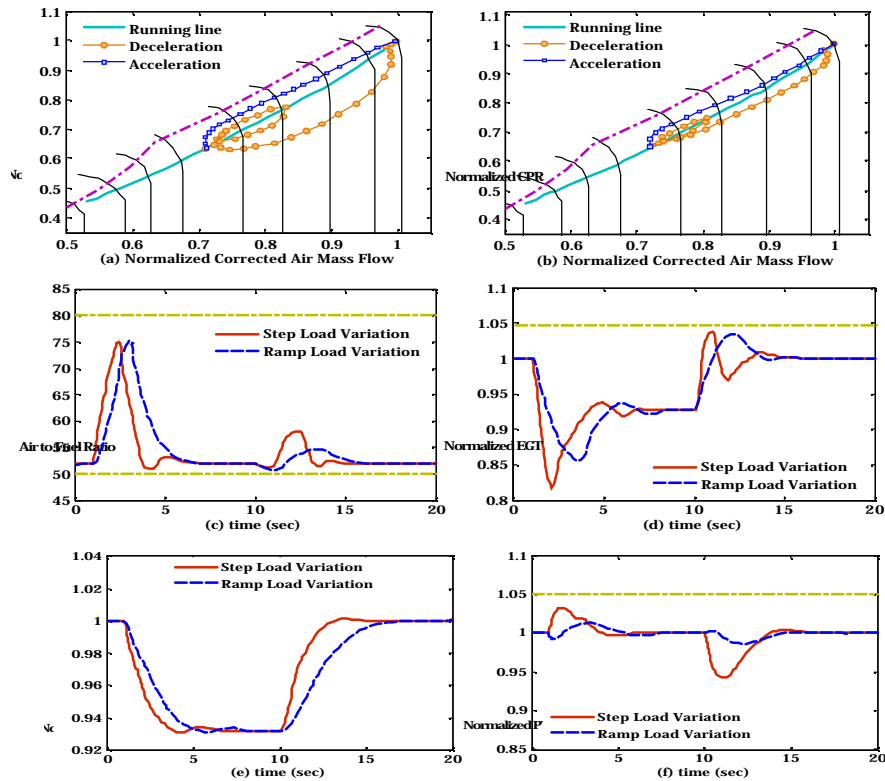


Fig 7: Transient simulation results in presence of min-max controller: a) CPR vs. corrected air mass flow for step load variations; b) CPR vs corrected air mass flow for ramp load variations; c) Air to fuel ratio; d) Normalized EGT; e) Normalized gas generator shaft speed; f) Normalized power turbine shaft speed

in acceleration mode. Figure 7c illustrates variations of air to fuel ratio during transient operation of the system. The range of variations of this property must not overpass the limitations. If the air to fuel ratio exceeds upper limit, flame-out will occur and if this value crosses lower limit, the compressor is exposed to aerodynamic instability and flame-out might also occur due to the richness of air and fuel composition. The gas generator acceleration and

deceleration control loops are in charge of maintaining desired air to fuel ratio. Figure 7d shows the variations of exhaust gas temperature. High values of exhaust temperature indicate high internal temperature which leads to turbine blade damage. The EGT control loop is charged to keep exhaust temperature within desired boundaries. The results obtained demonstrate that the controller has succeeded in satisfying the engine operational and

physical constraints within desired range. Time plots of the rotational speed of gas generator and power turbine are illustrated in Fig. 7e, f, respectively. By rejection of load, power turbine's shaft speed increases. In order to keep the power turbine speed at design value, the controller reduces the amount of fuel fed to the engine. As the load rises, the amount of fuel mass flow is increased to prevent power turbine speed reduction. Whenever a variation in load command happens, it is the role of power turbine speed and acceleration control loops to return rotational speed to its design value. It can be inferred from the results shown in Fig. 7f that the controller is capable of meeting the requirements.

To summarize the operation of the suggested model in transient mode, at the beginning of simulation when the gas turbine is operating at design conditions, the variable inlet guide vanes are completely open, letting the entire air flow through compressor inlet. At this point, all the properties of gas are equal to design values. When a load rejection of 50% occurs at $t = 2$ sec, the power turbine rotational speed increases and the control system reduces the amount of fuel fed to the gas turbine. This leads to increase in the amount of air to fuel ratio and enhances the risk of flame-out. In this way, the controller changes the VIGV position and thereby reduces the air mass flow in order to prevent the flame-out.

When a 50% rise is applied to load signal, the power turbine speed drops instantaneously. At this time, VIGVs and fuel flow are used simultaneously to change the speed. Increase in fuel flow at a greater rate than the gas generator speed will decrease the air to fuel ratio and thus increase the risk of flame-out and aerodynamic instability. The gas generator speed and acceleration control loops preserve the engine from overpassing the operational limitations. In acceleration mode, since air and fuel flows are varying at the similar rate, sudden raise in gas temperature occurs but the exhaust gas temperature control loop keeps it at desired range.

CONCLUSION

In this study, modeling, simulation and control of the industrial two-shaft gas turbines has been presented. The suggested model is based on zero-dimensional conservation equations applied to each component of the engine for design point, steady-state and transient operational conditions. The validation against steady-state performance data is satisfactory and indicates reliability of the suggested model. A fuel control system based on min-max control strategy has been

designed and its parameters are optimized using invasive weed optimization algorithm. The multi-loop controller has proved to satisfy the control requirements in sharp loading and unloading conditions.

REFERENCES

- Breikin, T.V., V.Y. Arkov and G.G. Kulikov, 2004. Regularisation approach for real-time modelling of aero gas turbines. *Control Eng. Pract.*, 12: 401-407.
- Camporeale, S.M., B. Fortunato and A. Dumas, 1997. Non-linear simulation model and multivariable control of a regenerative single shaft gas turbine. *Proceedings of the 1997 IEEE International Conference on Control Applications*, October 5-7, 1997, Hartford, CT., USA., pp: 721-723.
- Camporeale, S.M., B. Fortunato and A. Dumas, 2000. Dynamic modelling of recuperative gas turbines. *J. Power Energy*, 214: 213-225.
- Camporeale, S.M., B. Fortunato and M.A. Mastrovito, 2002. A modular code for real time dynamic simulation of gas turbines in Simulink. *J. Eng. Gas Turbines Power*, 128: 506-517.
- Chacartegui, R., D. Sanchez, A. Munoz and T. Sanchez, 2011. Real time simulation of medium size gas turbines. *Energy Conv. Manage.*, 52: 713-724.
- Chipperfield, A. and P. Fleming, 1996. Multiobjective gas turbine engine controller design using genetic algorithms. *IEEE Trans. Ind. Electron.*, 43: 583-587.
- Cohen, H., G. Rogers and H. Saravanamuttoo, 1966. *Gas Turbine Theory*. Longman Group Ltd., London, UK.
- Fawke, A.J., H. Saravanamuttoo and M. Holmes, 1972. Experimental verification of a digital computer simulation method for predicting gas turbine dynamic behaviour. *Inst. Mech. Eng.*, 186: 323-329.
- Gilani, S.I.H., A.T. Baheta and C. Rangkuti, 2009. Study the effect of variable vanes on performance of axial compressor for single shaft gas turbine cogeneration plant. *Proceedings of the 3rd International Conference on Energy and Environment*, December 7-8, 2009, Malacca, pp: 40-44.
- Jafari, S. and M. Montazeri-Gh, 2011. Evolutionary optimization for gain tuning of jet engine min-max fuel controller. *J. Propulsion Power*, 27: 1015-1023.
- Jafarian, K., M. Mobin and Z. Honarkar, 2016. Predictive control design of gas turbine using multi-objective optimization approach. *Proceedings of the 2016 6th International Conference on Industrial Engineering and Operations Management*, March 8-10, 2016, Kuala Lumpur, Malaysia -.

- Kim, J.H., T.W. Song, T.S. Kim and S.T. Ro, 2001a. Model development and simulation of transient behavior of heavy duty gas turbines. *J. Eng. Gas Turbines Power*, 123: 589-594.
- Kim, J.H., T.S. Kim and S.T. Ro, 2001b. Analysis of the dynamic behaviour of regenerative gas turbines. *J. Power Energy*, 215: 339-346.
- Kim, J.H., T.W. Song and T.S. Kim, 2002. Dynamic simulation of full startup procedure of heavy-duty gas turbines. *J. Eng. Gas Turbines Power*, 124: 510-516.
- Komaki, M., M. Mobin, E. Teymourian and M. Sheikh, 2015. A general variable neighborhood search algorithm to minimize makespan of the distributed permutation flowshop scheduling problem. *Proceedings of the 17th International Conference on Innovation, Engineering Management and Technology*, January 26-27, 2015, Istanbul, Turkey -.
- Li, Z., M. Mobin and T. Keyser, 2016. Multi-objective and multi-stage reliability growth planning in early product-development stage. *IEEE Trans. Reliab.*, 65: 769-781.
- Lichtsinder, M. and Y. Levy, 2006. Jet engine model for control and real-time simulations. *J. Eng. Gas Turbines Power*, 128: 745-753.
- Mehrabian, A.R. and C. Lucas, 2006. A novel numerical optimization algorithm inspired from weed colonization. *Ecol. Inform.*, 1: 355-366.
- Mehrian, S.H.Z., S.A.R. Amrei and M. Maniat, 2016. Structural health monitoring using optimizing algorithms based on flexibility matrix approach and combination of natural frequencies and mode shapes. *Int. J. Struct. Eng.*, Vol. 7, No. 4.
- Mehrian, S.M., A.R. Daneshmehr, A. Hadi, A. Atf and S.Z. Mehrian, 2013. Presentation of new model to calculate strain energy release rate for a crack in composite structure. *Caspian J. Applied Sci. Res.*, 2: 26-34.
- Mehrian, S.M.N. and S.Z. Mehrian, 2015. Modification of space truss vibration using piezoelectric actuator. *Applied Mech. Mater.*, 811: 246-252.
- Mobin, M., Z. Li and M.M. Khoraskani, 2015. Multi-objective X-bar control chart design by integrating NSGA-II and data envelopment analysis. *Proceedings of the 2015 Industrial and Systems Engineering Research Conference*, May 30-June 2, 2015, Nashville, TN., USA -.
- Mohammadi, E. and M. Montazeri-Gh, 2014. A new approach to the gray-box identification of wiener models with the application of gas turbine engine modeling. *J. Eng. Gas Turbines Power*, Vol. 137. 10.1115/1.4029170
- Mohammadi, E., M. Montazeri-Gh and P. Khalaf, 2013. Metaheuristic design and optimization of fuzzy-based gas turbine engine fuel controller using hybrid invasive weed optimization/particle swarm optimization algorithm. *J. Eng. Gas Turbines Power*, Vol. 136. 10.1115/1.4025884
- Montazeri-Gh, M., E. Mohammadi and S. Jafari, 2011. Fuzzy-based gas turbine engine fuel controller design using particle swarm optimization. *Applied Mech. Mater.*, 110-116: 3215-3222.
- Navrotsky, V. and M. Blomstedt, 2008. Continued enhancement of SGT-600 gas turbine design and maintenance. *Proceedings of the ASME Industrial and Cogeneration Conference*, June 9-13, 2008, Berlin, Germany, pp: 285-293.
- Nelson, G.M. and H. Lakany, 2007. An investigation into the application of fuzzy logic control to industrial gas turbines. *J. Eng. Gas Turbines Power*, 129: 1138-1142.
- Nordstrom, L., 2005. Construction of a simulator for the Siemens gas turbine SGT-600. Linkoping University, Department of Electrical Engineering, Sweden.
- Nowruzpour Mehrian, S.M., A. Nazari and M.H. Naei, 2014. Coupled thermoelasticity analysis of annular laminate disk using Laplace transform and Galerkin finite element method. *Applied Mech. Mater.*, 656: 298-304.
- Rao, S.V., D. Moellenhoff and J.A. Jaeger, 1990. Linear state variable dynamic model and estimator design for allison T406 gas turbine engine. *Int. J. Turbo Jet Eng.*, 7: 179-186.
- Rowen, W.I., 1983. Simplified mathematical representations of heavy-duty gas turbines. *J. Eng. Power*, 105: 865-869.
- Saravanamuttoo, H. and A.J. Fawke, 1970. Simulation of gas turbine dynamic performance. *Proceedings of the ASME Gas Turbine Conference and Products Show*, May 24-28, 1970, Brussels, Belgium, pp: 1-8.
- Schetzen, M., 1981. Nonlinear system modeling based on the wiener theory. *Proc. IEEE*, 69: 1557-1573.
- Tavana, M., Z. Li, M. Mobin, M. Komaki and E. Teymourian, 2016. Multi-objective control chart design optimization using NSGA-III and MOPSO enhanced with DEA and TOPSIS. *Expert Syst. Applic.*, 50: 17-39.

- Turie, S.E., 2011. Gas turbine plant modeling for dynamic simulation. M.Sc. Thesis, KTH School of Industrial Engineering and Management, Department of Energy Technology, Stockholm.
- Vafadamikjoo, A., M. Khatami, M. Mobin and A. Roshani, 2015. A meta-heuristic approach to locate optimal switch locations in cellular mobile networks. Proceedings of the 2015 American Society of Engineering Management Conference, October 7-10, 2015, Indianapolis, Indiana-.
- Walsh, P.P. and P. Fletcher, 2004. Gas Turbine Performance. 2nd Edn., Blackwell Science Ltd., New York, USA., ISBN-13: 9780632064342, Pages: 664.
- Wang, J., C. Zhang and Y. Jing, 2008. Adaptive PID control with BP neural network self-tuning in exhaust temperature of micro gas turbine. Proceedings of the 3rd IEEE Conference on Industrial Electronics and Applications, June 3-5, 2008, Singapore, pp: 532-537.